# Supplementary material for LHCb-PAPER-2020-009

## Breit–Wigner mass of the $\chi_{c1}(3872)$ state

The precision of the mass measurement made here is similar to that found in the analysis using a sample of detached $\chi_{c1}(3872) \to J/\psi\,\pi^+\pi^-$ decays produced in b-hadron decays [1]. That analysis is based on the $(15.63 \pm 0.38) \times 10^3$ signal candidates and finds

$$m_{\chi_{c1}(3872)} - m_{\psi(2S)} = 185.598 \pm 0.067 \pm 0.068\,\text{MeV}/c^2\,, \tag{S1}$$

where the first uncertainty is statistical and the second is systematic. The dominant systematic uncertainty arises from the knowledge of the momentum scale. The result of Ref. [1] is averaged with the mass difference of $185.488 \pm 0.062 \pm 0.030\,\text{MeV}/c^2$ [2]. The small statistical overlap between the samples is taken into account by removing the events that are common between the two studies from the inclusive analysis. This increases the statistical uncertainty on the analysis of Ref. [1] to $0.069\,\text{MeV}/c^2$. In the averaging procedure the uncertainties due to the momentum scale are assumed to be fully correlated. The average of the two LHCb measurements is

$$m_{\chi_{c1}(3872)} - m_{\psi(2S)} = 185.542 \pm 0.060\,\text{MeV}/c^2\,. \tag{S2}$$

This is converted into an estimate of the $\chi_{c1}(3872)$ mass using the value $m_{\psi(2S)} = 3686.097 \pm 0.010\,\text{MeV}/c^2$ [3] to give

$$m_{\chi_{c1}(3872)} = 3871.639 \pm 0.060 \pm 0.010\,\text{MeV}/c^2\,,$$

where the second uncertainty is due to the knowledge of the $\psi(2S)$ mass. This measured mass has been averaged with the previous measurements summarized in the PDG. This new world average

$$m_{\chi_{c1}(3872)}\big|_{\text{WA}} = 3871.64 \pm 0.06\,\text{MeV}/c^2\,, \tag{S3}$$

is shown in Fig. S1 as an orange band. Also included on this plot is a comparison with $m_{\text{D}^0} + m_{\text{D}^{*0}}$ which is calculated to be [1]

$$m_{\text{D}^0} + m_{\text{D}^{*0}} = 3871.704 \pm 0.110\,\text{MeV}/c^2\,, \tag{S4}$$

using the values in Ref. [3]. Correlations due to the knowledge of the charged and neutral kaon masses between the measurements have been taken into account. The difference between the $m_{\chi_{c1}(3872)}$ mass and the $\text{D}^0\text{D}^{*0}$ threshold,

$$\delta E \equiv (\,\text{m}_{\text{D}^0} + m_{\text{D}^{*0}})\,c^2 - m_{\chi_{c1}(3872)}c^2\,,$$

is computed to be

$$\delta E|_{\text{LHCb}} = 66 \pm 124\,\text{keV}\,. \tag{S5}$$

Including all available data $\delta E$ is determined as

$$\delta E|_{\text{ALL}} = 60 \pm 122\,\text{keV}\,. \tag{S6}$$

The uncertainty is dominated by the knowledge of the neutral and charged kaon masses [3]. The compilation of the measurements of the $\chi_{c1}(3872)$ mass is presented in Fig. S1 and Table S1.

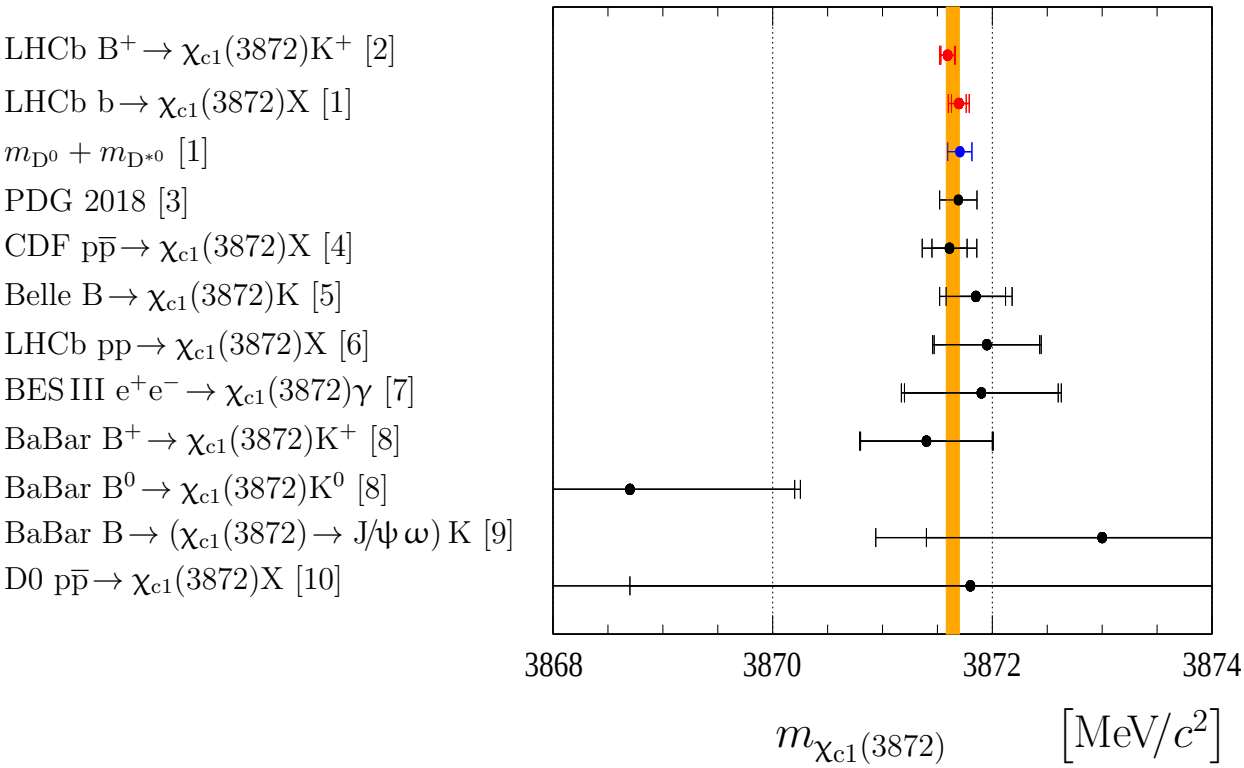


Figure S1: Measurements of the Breit–Wigner mass of the $\chi_{c1}(3872)$ state. The inner error bars indicate the statistical uncertainty, and the outer error bars correspond to the quadratic sum of the statistical and systematic uncertainties. A sum of $D^0$ and $D^{*0}$ masses, $m_{D^0} + m_{D^{*0}}$, is shown with blue color. The orange band represents the value and the uncertainty on world average of the $\chi_{c1}(3872)$ mass measurements including the new LHCb results.

Table S1: Measurements of the mass of the $\chi_{c1}(3872)$ state. The third uncertainty is due to the finite knowledge of $\psi(2S)$ mass.

| Experiment | | | $m_{\chi_{c1}(3872)}$ [ MeV/$c^2$] |
|---|---|---|---|
| LHCb | [1] | $b \to \chi_{c1}(3872)X$ | $3871.695 \pm 0.067 \pm 0.068 \pm 0.010$ |
| LHCb | [2] | $B^+ \to \chi_{c1}(3872)K^+$ | $3871.593 \pm 0.062 \pm 0.031 \pm 0.010$ |
| LHCb average | | | $3871.639 \pm 0.060 \pm 0.010$ |
| $m_{D^0} + m_{D^{*0}}$ | [1] | | $3871.70 \pm 0.11$ |
| PDG 2018 | [3] | | $3871.69 \pm 0.17$ |
| CDF | [4] | $p\overline{p} \to \chi_{c1}(3872)X$ | $3871.61 \pm 0.16 \pm 0.19$ |
| Belle | [5] | $B \to \chi_{c1}(3872)K$ | $3871.85 \pm 0.27 \pm 0.19$ |
| LHCb | [6] | $pp \to \chi_{c1}(3872)X$ | $3871.95 \pm 0.48 \pm 0.12$ |
| BES III | [7] | $e^+e^- \to \gamma\chi_{c1}(3872)$ | $3871.9 \pm 0.7 \pm 0.2$ |
| BaBar | [8] | $B^+ \to \chi_{c1}(3872)K^+$ | $3871.4 \pm 0.6 \pm 0.1$ |
| BaBar | [8] | $B^0 \to \chi_{c1}(3872)K^0$ | $3868.7 \pm 1.5 \pm 0.4$ |
| BaBar | [9] | $B \to (\chi_{c1}(3872) \to J/\psi\,\omega)\,K$ | $3873.0 \,^{+\ 1.8}_{-\ 1.6} \pm 1.3$ |
| D0 | [10] | $p\overline{p} \to \chi_{c1}(3872)X$ | $3871.8 \pm 3.1 \pm 3.0$ |
| Our average | | | $3871.64 \pm 0.06$ |

## Breit–Wigner width of the $\chi_{c1}(3872)$ state

The compilation of the measurements and upper limits on the Breit–Wigner width of the $\chi_{c1}(3872)$ state is presented in Fig. S2 and Table S2.

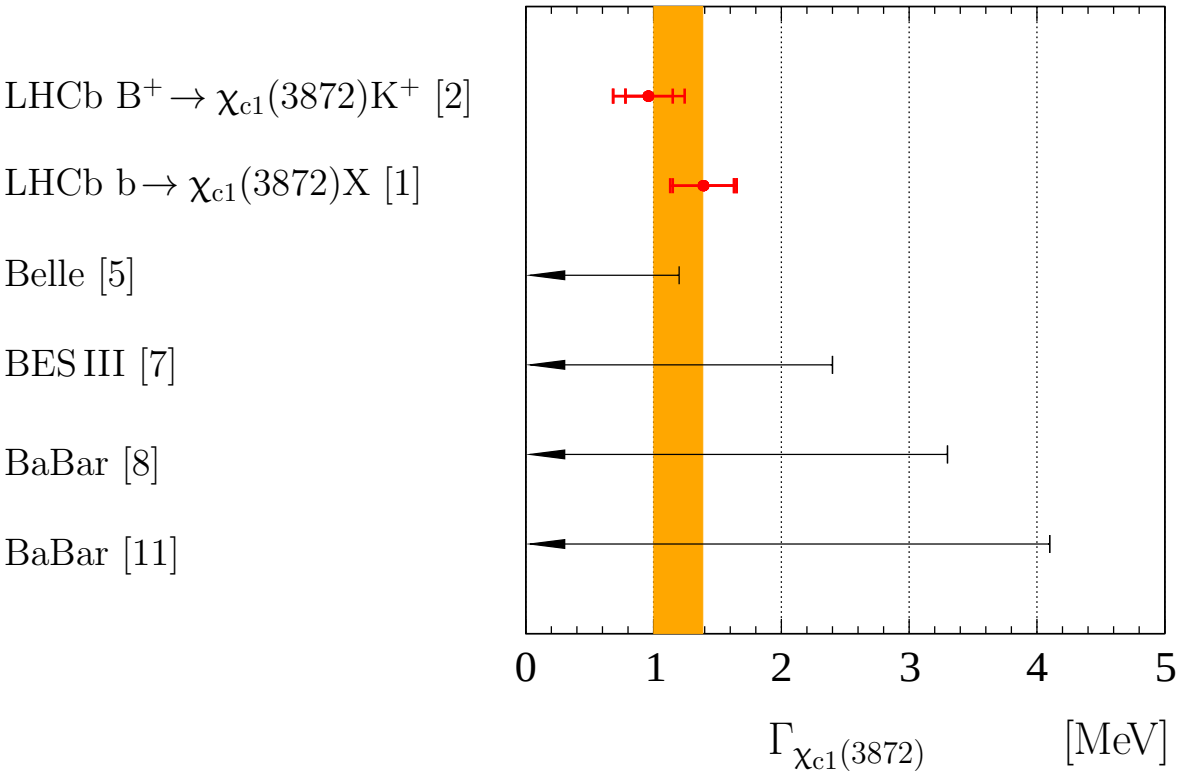


Figure S2: The measurements and upper limits of the Breit–Wigner width of the $\chi_{c1}(3872)$ state. The upper limits are at 90% CL. The inner error bars indicate the statistical uncertainty while the outer error bars correspond to the quadratic sum of the statistical and systematic uncertainties. The orange band shows the weighted average.

Table S2: The measurements and upper limits of the Breit–Wigner width of the $\chi_{c1}(3872)$ state. The upper limits are at 90% CL.

| Experiment | | | $\Gamma_{\chi_{c1}(3872)}$ [MeV] |
|---|---|---|---|
| Belle | [5] | $B \to \chi_{c1}(3872)K$ | $< 1.2$ |
| BES III | [7] | $e^+e^- \to \chi_{c1}(3872)\gamma$ | $< 2.4$ |
| BaBar | [8] | $B \to \chi_{c1}(3872)K$ | $< 3.3$ |
| BaBar | [11] | $B \to \chi_{c1}(3872)K$ | $< 4.1$ |
| LHCb | [1] | $b \to \chi_{c1}(3872)X$ | $1.39 \pm 0.24 \pm 0.10$ |
| LHCb | [2] | $B^+ \to \chi_{c1}(3872)K^+$ | $0.96 \,^{+\,0.19}_{-\,0.18} \pm 0.21$ |
| Our average | | | $1.19 \pm 0.19$ |

## The mass of the $\psi_2(3823)$ state

The compilation of the measurements of the mass of the $\psi_2(3823)$ state is presented in Fig. S3 and Table S3.

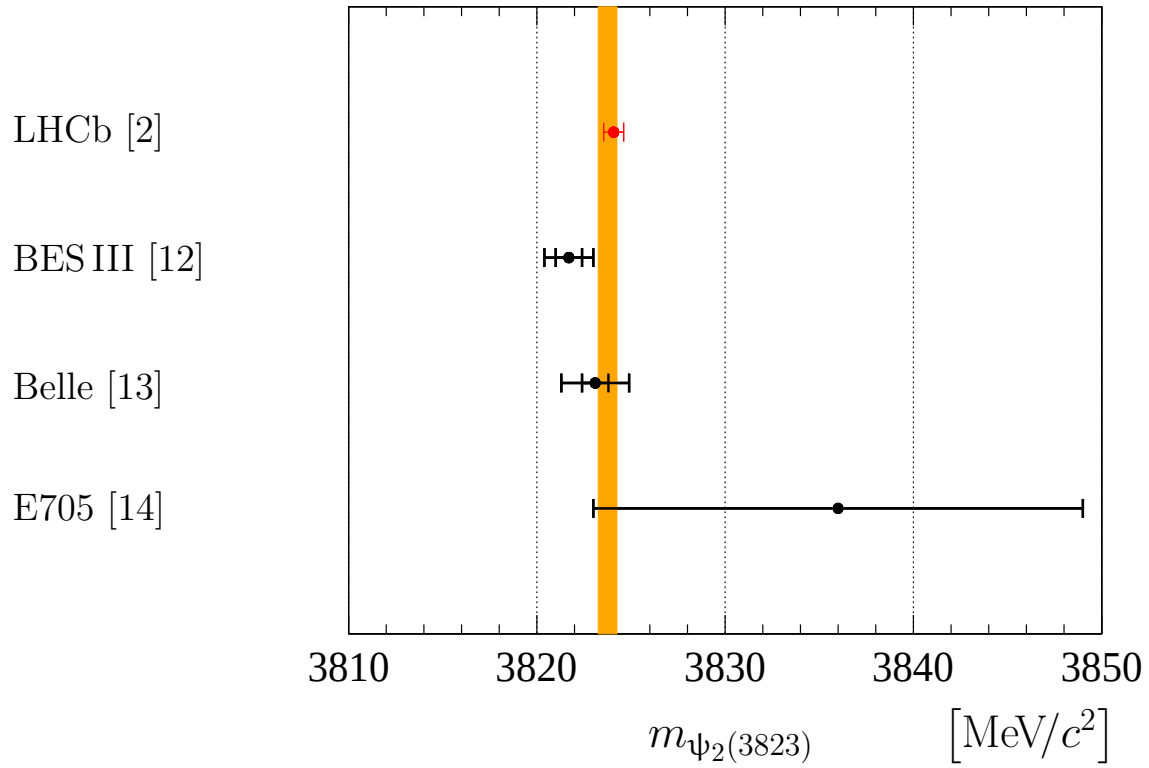


Figure S3: The measurements of the mass of the $\psi_2(3823)$ state. The error bars indicate the total uncertainty (quadratic sum of all components) and the inner bars (when shown) correspond to the statistical uncertainty. The orange band shows the weighted average.

Table S3: The measurements of the mass of the $\psi_2(3823)$ state. The third uncertainty is due to knowledge of $\psi(2S)$ mass.

| Experiment | | | $m_{\psi_2(3823)}$ $[\mathrm{MeV}/c^2]$ |
|---|---|---|---|
| BES III | [12] | $e^+e^- \to (\psi_2(3823) \to \chi_{c1}\gamma)\,\pi^+\pi^-$ | $3821.7 \pm 1.3 \pm 0.7$ |
| Belle | [13] | $B \to (\psi_2(3823) \to \chi_{c1}\gamma)\,K$ | $3823.1 \pm 1.8 \pm 0.7$ |
| E705 | [14] | $\pi^{\pm}\mathrm{Li} \to (\psi_2(3823) \to J/\psi\,\pi^+\pi^-)\,X$ | $3836 \pm 13$ |
| PDG 2018 | [3] | | $3822.2 \pm 1.2$ |
| LHCb | [2] | $B^+ \to (\psi_2(3823) \to J/\psi\,\pi^+\pi^-)\,K^+$ | $3824.08 \pm 0.53 \pm 0.14 \pm 0.01$ |
| Our average | | | $3823.76 \pm 0.50$ |

### $\mathcal{B}_{B^+\to\chi_{c1}(3872)K^+} \times \mathcal{B}_{\chi_{c1}(3872)\to J/\psi\pi^+\pi^-}$

The product of the branching fractions $\mathcal{B}_{B^+\to\chi_{c1}(3872)K^+} \times \mathcal{B}_{\chi_{c1}(3872)\to J/\psi\pi^+\pi^-}$ is computed from the measured ratio $\mathcal{R}^{\chi_{c1}(3872)}_{\psi(2S)}$, using the known values of branching fractions [3]:

$$\begin{aligned} \mathcal{B}_{B^+\to\psi(2S)K^+} &= (\ 6.21 \pm 0.22) \times 10^{-4}\,, \\ \mathcal{B}_{\psi(2S)\to J/\psi\pi^+\pi^-} &= (34.68 \pm 0.30) \times 10^{-2}\,. \end{aligned}$$

The compilation of the measurements is presented in Fig. S4 and Table S4.

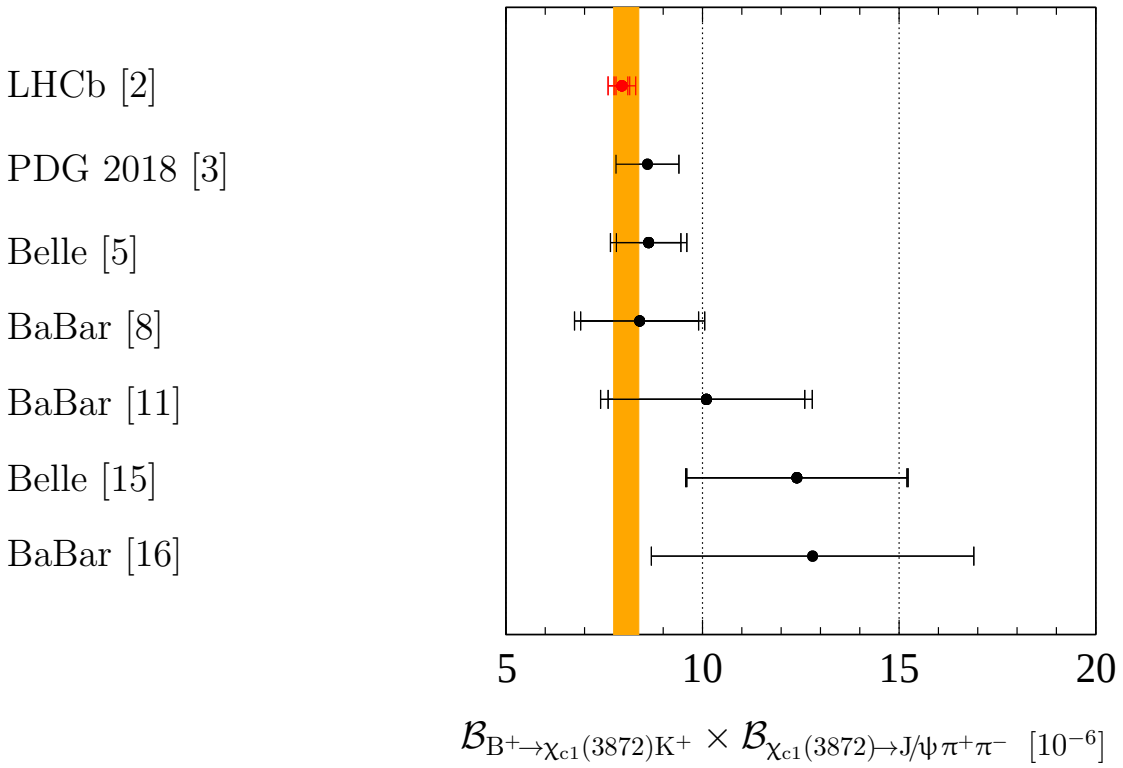


Figure S4: The measurements of the product of branching fractions for $B^+ \to \chi_{c1}(3872)K^+$ and $\chi_{c1}(3872) \to J/\psi\pi^+\pi^-$ decays. The innermost error bars indicate the statistical uncertainty, and the second (outer) error bars correspond to the sum in quadrature of the statistical and systematic uncertainties. For the LHCb point (in red), a third set of error bars are shown that include the uncertainties associated with the $B^+ \to \psi(2S)K^+$ and $\psi(2S) \to J/\psi\pi^+\pi^-$ branching fractions. The orange band shows the weighted average.

Table S4: The measurements of the product of branching fractions $\mathcal{B}_{B^+\to\chi_{c1}(3872)K^+}$ and $\mathcal{B}_{\chi_{c1}(3872)\to J/\psi\pi^+\pi^-}$. The PDG'18 average includes only the measurements from Refs. [5, 8]. The third uncertainty for the LHCb measurement is due to the knowledge of $\mathcal{B}_{B^+\to\psi(2S)K^+}$ and $\mathcal{B}_{\psi(2S)\to J/\psi\pi^+\pi^-}$.

| Experiment | | $\mathcal{B}_{B^+\to\chi_{c1}(3872)K^+} \times \mathcal{B}_{\chi_{c1}(3872)\to J/\psi\pi^+\pi^-}$ $[10^{-6}]$ |
|---|---|---|
| Belle | [5] | $8.63 \pm 0.82 \pm 0.52$ |
| BaBar | [8] | $8.4 \pm 1.5 \pm 0.7$ |
| BaBar | [11] | $10.1 \pm 2.5 \pm 1.0$ |
| BaBar | [16] | $12.8 \pm 4.1$ |
| Belle | [15] | $12.4 \pm 2.8 \pm 0.4$ |
| PDG 2018 | [3] | $8.6 \pm 0.8$ |
| LHCb | [2] | $7.95 \pm 0.15 \pm 0.13 \pm 0.29$ |
| Our average | | $8.06 \pm 0.32$ |

### $\mathcal{B}_{B^+\to\psi_2(3823)K^+}$

The branching fraction for the decay $B^+ \to \psi_2(3823)K^+$ is calculated from the measured ratio $\mathcal{R}^{\psi_2(3823)}_{\psi(2S)}$, using the known values of branching fractions for the $B^+ \to \psi(2S)K^+$ and $\psi(2S) \to J/\psi\pi^+\pi^-$ decays [3] and taking $\mathcal{B}_{\psi_2(3823)\to J/\psi\pi^+\pi^-}$ as $\frac{2}{3}\mathcal{B}_{\psi_2(3823)\to J/\psi\pi\pi}$ with $\mathcal{B}_{\psi_2(3823)\to J/\psi\pi\pi} = 34\%$ [17]. The measurement of $\mathcal{B}_{B^+\to\psi_2(3823)K^+} \times \mathcal{B}_{\psi_2(3823)\to\chi_{c1}\gamma} = (9.7 \pm 2.8 \pm 1.1) \times 10^{-6}$ by the Belle collaboration [13] together with computed value of $\mathcal{B}_{\psi_2(3823)\to\chi_{c1}\gamma} = 46\%$ [17] is used for comparison. The compilation of the measurements is presented in Fig. S5 and Table S5. The predicted range $75 \le \Gamma_{\psi_2(3823)\to J/\psi\pi^+\pi^-} \le 125\,\text{keV}$ [18] results in additional 17% and 10% uncertainty for the measurements of the $\mathcal{B}_{B^+\to\psi_2(3823)K^+}$ derived from the LHCb and Belle results, respectively.

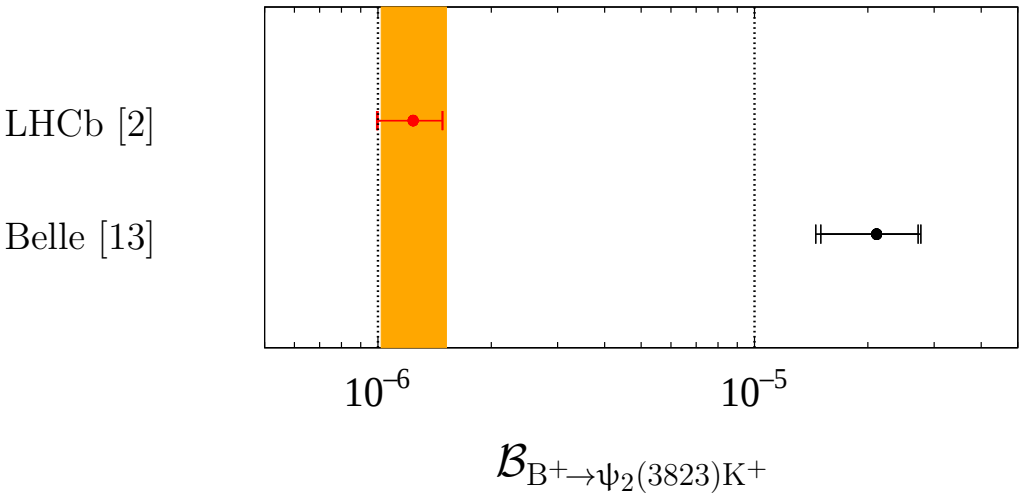


Figure S5: Evaluations of the branching fraction $\mathcal{B}_{B^+\to\psi_2(3823)K^+}$. The error bars indicate the total uncertainty (quadratic sum of all components), the inner bars (when shown) correspond to statistical uncertainty. No uncertainty due to $\mathcal{B}_{\psi_2(3823)\to J/\psi\pi^+\pi^-}$ and $\mathcal{B}_{\psi_2(3823)\to\chi_{c1}\gamma}$ is accounted for. The orange band shows the weighted average.

Within a factorization approach the branching fraction for the decay $B^+ \to \psi_2(3823)K^+$ vanishes, and a large value for this branching fraction requires a significant contribution of the $D_s^{(*)+}\overline{D}^{(*)0}$ rescattering amplitudes in the $B^+ \to c\bar{c}K^+$ decays [17]. If the result by the Belle collaboration for the $\mathcal{B}_{B^+\to\psi_2(3823)K^+} \times \mathcal{B}_{\psi_2(3823)\to\chi_{c1}\gamma}$ [13] and the calculations for the $\psi_2(3823) \to \chi_{c1}\gamma$ and $\psi_2(3823) \to J/\psi\pi^+\pi^-$ branching fractions [17] were correct, the expected number of signal $B^+ \to (\psi_2(3823) \to J/\psi\pi^+\pi^-)K^+$ decays at LHCb is $2300 \pm 700$ instead of the observed number of $137 \pm 26$. Similarly, the value of $\mathcal{B}_{B^+\to\psi_2(3823)K^+}$ derived from the LHCb measurement [2] and $\psi_2(3823) \to J/\psi\pi^+\pi^-$ branching fractions [17] implies that no $B^+ \to (\psi_2(3823) \to \chi_{c1}\gamma)K^+$ signal should be visible in the analysis, while $33.2 \pm 9.7$ signal candidates are observed [13]. The contradiction can be resolved if the ratio of the partial widths $\mathfrak{R}_{\psi_2(3823)}$,

$$\mathfrak{R}_{\psi_2(3823)} \equiv \frac{\Gamma_{\psi_2(3823)\to J/\psi\pi^+\pi^-}}{\Gamma_{\psi_2(3823)\to\chi_{c1}\gamma}},$$

is significantly smaller than the value of about 0.5 derived in Ref. [17]. The good agreement for the ratio $\mathcal{R}^{\chi_{c1}(3872)}_{\psi(2S)}$, and the derived product of the branching fractions

for the $B^+ \to \chi_{c1}(3872)K^+$ and $\chi_{c1}(3872) \to J/\psi\,\pi^+\pi^-$ decays with their known values [3] supports the $\mathcal{R}^{\psi_2(3823)}_{\psi(2S)}$ ratio the obtained in the present analysis and the derived product of the branching fractions.

Table S5: Evaluations of the branching fraction for the $B^+ \to \psi_2(3823)K^+$ decay. The third uncertainty for LHCb measurement is due to knowledge of branching fractions for the $B^+ \to \psi(2S)K^+$ and $\psi(2S) \to J/\psi\,\pi^+\pi^-$ decays. No uncertainty due to $\mathcal{B}_{\psi_2(3823)\to J/\psi\,\pi^+\pi^-}$ and $\mathcal{B}_{\psi_2(3823)\to\chi_{c1}\gamma}$ is included.

| Experiment | | $\mathcal{B}_{B^+\to\psi_2(3823)K^+}$ |
|---|---|---|
| Belle | [13] | $(2.11 \pm 0.61 \pm 0.24) \times 10^{-5}$ |
| LHCb | [2] | $(1.24 \pm 0.24 \pm 0.04 \pm 0.05) \times 10^{-6}$ |
| Our average | | $(1.27 \pm 0.25) \times 10^{-6}$ |

## Interference effects for the $\chi_{c1}(3872)$ parameters

The background-subtracted $J/\psi\pi^+\pi^-$ mass distribution is used to study interference effects for the $\chi_{c1}(3872)$ parameters. The *sPlot* technique is used for background subtraction using $m_{J/\psi\pi^+\pi^-K^+}$ as the discriminating variable [19]. The distribution is fit with a function that accounts for the signal, coherent and incoherent background

$$\mathcal{F}(m) = \mathcal{N}\left(\left|\mathcal{A}_{\rm BW}(m) + b_{\rm c}(m)\,e^{i\delta(m)}\right|^2 \circledast \mathfrak{R}\right) + b_{\rm i}^2(m)\,, \tag{S7}$$

where $\mathcal{A}_{\rm BW}(m)$ is a Breit–Wigner amplitude, convolved with the detector resolution function $\mathfrak{R}$, and $\mathcal{N}$ stands for a normalisation constant. The coherent and incoherent background components $b_{\rm c}(m)$ and $b_{\rm i}^2(m)$ are parameterised with positive polynomial functions, and the relative interference phase $\delta(m)$ is taken to be constant for the narrow $3.85 \leq m_{J/\psi\pi^+\pi^-} < 3.90\,\text{GeV}/c^2$ region, $\delta(m) \equiv \delta_0$. Equally good description of data is achieved for totally incoherent ($b_{\rm c}(m) \equiv 0$) and coherent ($b_{\rm i}^2(m) \equiv 0$) background hypotheses, see Fig. S6, as well as for any intermediate scenario with the relative phase $\delta_0$ close to $\frac{\pi}{2}$. The latter reflects a high symmetry of the observed $\chi_{c1}(3872)$ lineshape. For all scenarios variations of the mass and width-parameter are limited to $50\,\text{keV}/c^2$ and $150\,\text{keV}$, respectively.

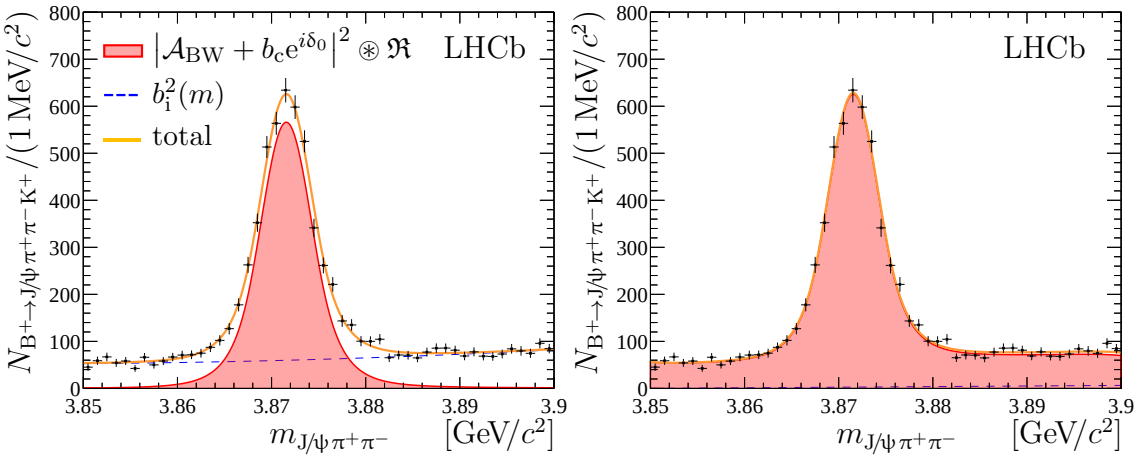


Figure S6: Background-subtracted $J/\psi\pi^+\pi^-$ mass distribution from signal $B^+ \to J/\psi\pi^+\pi^-K^+$ decays with overlaid fit results with (left) incoherent ($b_{\rm c}(m) \equiv 0$) and (right) coherent ($b_{\rm i}^2(m) \equiv 0$) background parameterisation.

# References


[1] LHCb collaboration, R. Aaij *et al.*, *Study of the lineshape of the* $\chi_{c1}(3872)$ *meson*, arXiv:2005.13419, submtted to Phys. Rev. D.

[2] LHCb collaboration, R. Aaij *et al.*, *Study of the* $\psi_2(3823)$ *and* $\chi_{c1}(3872)$ *states in the* $B^+ \to (J/\psi\,\pi^+\pi^-)\,K^+$ *decays* , arXiv:2005.13422, submitted to JHEP.

[3] Particle Data Group, M. Tanabashi *et al.*, *Review of particle physics*, Phys. Rev. **D98** (2018) 030001, and 2019 update.

[4] CDF collaboration, T. Aaltonen *et al.*, *Precision measurement of the* X(3872) *mass in* $J/\psi\,\pi^+\pi^-$ *decays*, Phys. Rev. Lett. **103** (2009) 152001, arXiv:0906.5218.

[5] Belle collaboration, S.-K. Choi *et al.*, *Bounds on the width, mass difference and other properties of* $X(3872) \to \pi^+\pi^- J/\psi$ *decays*, Phys. Rev. **D84** (2011) 052004, arXiv:1107.0163.

[6] LHCb collaboration, R. Aaij *et al.*, *Observation of* X(3872) *production in* pp *collisions at* $\sqrt{s} = 7$ *TeV*, Eur. Phys. J. **C72** (2012) 1972, arXiv:1112.5310.

[7] BES III collaboration, M. Ablikim *et al.*, *Observation of* $e^+e^- \to \gamma X(3872)$ *at BES III*, Phys. Rev. Lett. **112** (2014) 092001, arXiv:1310.4101.

[8] BaBar collaboration, B. Aubert *et al.*, *Study of* $B \to X(3872)K$*, with* $X(3872) \to J/\psi\,\pi^+\pi^-$, Phys. Rev. **D77** (2008) 111101(R), arXiv:0803.2838.

[9] BaBar collaboration, P. del Amo Sanchez *et al.*, *Evidence for the decay* $X(3872) \to J/\psi\,\omega$, Phys. Rev. **D82** (2010) 011101(R), arXiv:1005.5190.

[10] D0 collaboration, V. M. Abazov *et al.*, *Observation and properties of the* X(3872) *decaying to* $J/\psi\,\pi^+\pi^-$ *in* $p\overline{p}$ *collisions at* $\sqrt{s} = 1.96$ *TeV*, Phys. Rev. Lett. **93** (2004) 162002, arXiv:hep-ex/0405004.

[11] BaBar collaboration, B. Aubert *et al.*, *Study of the* X(3872) *and* Y(4260) *in* $B^0 \to J/\psi\,\pi^+\pi^- K^0$ *and* $B^- \to J/\psi\,\pi^+\pi^- K^-$ *decays*, Phys. Rev. **D73** (2006) 011101(R), arXiv:hep-ex/0507090.

[12] BES III collaboration, M. Ablikim *et al.*, *Observation of the* $\psi(1^3D_2)$ *state in* $e^+e^- \to \pi^+\pi^-\gamma\chi_{c1}$ *at BES III*, Phys. Rev. Lett. **115** (2015) 011803, arXiv:1503.08203.

[13] Belle collaboration, V. Bhardwaj *et al.*, *Evidence of a new narrow resonance decaying to* $\chi_{c1}\gamma$ *in* $B \to \chi_{c1}\gamma K$, Phys. Rev. Lett. **111** (2013) 032001, arXiv:1304.3975.

[14] E705 collaboration, L. Antoniazzi *et al.*, *Search for hidden charm states decaying into* $J/\psi$ *or* $\psi'$ *plus pions*, Phys. Rev. **D50** (1994) 4258.

[15] Belle collaboration, S.-K. Choi *et al.*, *Observation of a narrow charmoniumlike state in exclusive* $B^\pm \to K^\pm\pi^+\pi^- J/\psi$ *decays*, Phys. Rev. Lett. **91** (2003) 262001, arXiv:hep-ex/0309032.

[16] BaBar collaboration, B. Aubert *et al.*, *Study of the* $B^- \to J/\psi K^- \pi^+ \pi^-$ *decay and measurement of the* $B^- \to X(3872) K^-$ *branching fraction*, Phys. Rev. **D71** (2005) 071103, arXiv:hep-ex/0406022.

[17] H. Xu, X. Liu, and T. Matsuki, *Understanding* $B^- \to X(3823) K^-$ *via rescattering mechanism and predicting* $B^- \to \eta_{c2}(^1D_2)/\psi_3(^3D_3) K^-$, Phys. Rev. **D94** (2016) 034005, arXiv:1605.04776.

[18] B. Wang *et al.*, *Using* $X(3823) \to J/\psi \pi^+ \pi^-$ *to identify coupled-channel effects*, Front. Phys. **11** (2016) 111402, arXiv:1507.07985.

[19] M. Pivk and F. R. Le Diberder, *sPlot: A statistical tool to unfold data distributions*, Nucl. Instrum. Meth. **A555** (2005) 356, arXiv:physics/0402083.